

Equal-Curvature Grazing Incidence X-Ray Telescopes

Timo T. Saha

NASA/Goddard Space Flight Center, Code 551, Greenbelt, MD 20771

William Zhang

NASA/Goddard Space Flight Center, Code 662, Greenbelt, MD 20771

We introduce a new type of x-ray telescope design; an Equal-Curvature telescope. We simply add a second-order axial sag to the base grazing incidence cone-cone telescope. The radius of curvature of the sag terms is the same on the primary surface and on the secondary surface. The design is optimized so that the on-axis image spot at the focal plane is minimized. The on-axis RMS spot diameter of two studied telescopes is less than 0.2 arc-seconds. The off-axis performance is comparable to equivalent Wolter type 1 telescopes.

OCIS codes: 340.7470, 340.7440, 220.1000, 220.2740

1. Introduction

This x-ray telescope design study was prompted by our desire to find more practical and cheaper telescopes for the Constellation-X mission (CSX)¹. The CSX observatory is comprised of 4 satellites. Each satellite has two telescopes on-board: the hard x-ray telescope (HXT) and the spectroscopic x-ray telescope (SXT)². The baseline SXT telescope design is nested Wolter type 1 design (W). The entrance aperture diameter is 1.6 m and the telescope axial focal length is 10 m. The mirrors can be up to 300 mm long. There are up to 167 mirror shells nested inside each other. The on-axis angular resolution requirement for the SXT telescopes is 15'' HPD at 1 KeV. The field of view (FOV) of the SXT telescope is limited to 1.25 arc-minutes.

Over the years several x-ray telescope configurations have been proposed. Wolter³ introduced paraboloid-hyperboloid type 1 designs. These designs have been widely used in x-ray astronomy. The W type 1 designs consist of paraboloidal primary mirror and confocal hyperboloidal secondary mirror. The telescope forms stigmatic on-axis image from infinite object. The telescope manufacturing errors always limit the on-axis image quality. This design has finite amount of coma⁴. Other large aberrations are the field curvature and fifth order oblique spherical aberration. Mangus and Underwood⁵ presented a detailed design study of W type 1 telescopes for solar applications. VanSpeybroeck and Chase⁶ have performed through design study of W type 1 telescopes including the nested designs.

Wolter-Schwarzschild⁷ (WS) designs offer the best image quality for narrow FOV applications. These designs are free of third order spherical aberration and coma. Chase and VanSpeybroeck⁸ have done the basic design study of these telescopes. The surfaces of the WS telescopes are complex functions of system parameters and are difficult to fabricate and test.

Optical designs for cone-cone type 1 telescopes have been designed and built^{9,10}. The advantage of this design is its simplicity. Since the telescope axial profiles do not have curvature, the focusing power of the design is very limited. In case of the CSX/SXT telescope, this aberration would consume large proportion of the resolution requirement.

Werner¹¹ studied and designed several polynomial x-ray telescopes. He compensated the on-axis spherical aberration against oblique spherical aberration. The resulting designs have more uniform resolution across the field of view. These designs are good for applications where large FOV is required. C.J. Burrows *et al*¹² and P.

Conconi *et al*¹³ have introduced specialized merit functions to optimize polynomial grazing incidence telescope for wide-field x-ray imaging.

Nariai^{14,15} designed a telescope consisting of 2 hyperboloids. In his designs spherical aberration is used to compensate oblique spherical aberration and coma is also minimized. Harvey¹⁶ used advanced features of ZEMAX lens design software to optimize hyperboloid-hyperboloid telescope for solar applications. These designs are excellent choices for missions where large FOV ($\sim 30 - 40$ arc-minutes) is required.

In this paper we introduce a new type of x-ray telescope. The cone-cone telescopes are easiest to fabricate and test. Unfortunately, these designs have very poor on-axis resolution. Our basic idea is to improve on-axis performance of the cone-cone design by introducing second order axial curvature to the surfaces of the cone-cone telescope. We also require that the curvature is the same both on the primary and secondary. The basic concept is shown in Figure 1. In Section II we present the basic equations for the design of cone-cone telescope. In Section III we introduce the surface equations of the Equal-Curvature (EC) telescope and show how these surfaces are derived from surfaces with purely spherical axial profiles. The derivation of basic parameters of the EC telescope is shown in Section IV. The equations include the derivation of an equation for the radius of curvature of the mirrors and show how it relates to basic system parameters. In Section V we introduce our analysis code (Optical Surface Analysis Code¹⁷), the surface equations of the OSAC code, and the principles we used to study the EC telescopes using the OSAC code.

In Section VI we present our study results for 2 EC designs (#1 and #2). The design #1 matches closely the size requirements of the CSX/SXT outer shell. The radial

height of this shell is 800 mm. The radial height of the design #2 is 200 mm. The grazing angles of this design are 4 times shallower than the grazing angles of the design #1.

2. Design of Cone-Cone Telescope

The cone-cone telescope is shown in Figure 1. This design consists of a primary cone and secondary cone. The intersection plane of the cones defines the system optical properties. The radial height (h_0) at this intersection plane and the axial distance (L) from this plane to the focal plane define the basic optical properties of the design. The third important design parameter is the grazing angle (i_{10}) incoming rays make with the surfaces. To optimize the telescope effective area, the grazing angle on the primary and the secondary are chosen to be equal. One needs also to select the axial lengths of the primary (L_1) and secondary (L_2) and the axial distances from the back of the primary to the intersection plane (c_1) and from the intersection plane to the secondary mirror (c_2).

Under these assumptions the design work is trivial. The surface equations of the primary ($j=1$) and secondary ($j=2$) in the telescope coordinate system can be expressed as:

$$h_j = h_0 - z_j \tan(i_{j0}). \quad (1)$$

If the grazing angles are identical on the surfaces, then the slope angle of the secondary is

$$i_{20} = 3 i_{10}.$$

Since the cone-cone telescope does not have a second or higher order component on the surface equations, the design cannot focus the rays in its radial cross-section. A collimated in-coming bundle of rays is bent towards the optical axis, but stays radially collimated. A ring of rays hitting the primary and secondary is focused to an on-axis point at different axial locations near the focal plane. The radial height of the image as a function the primary mirror radial height h_l is:

$$H = (h_l - h_0 - (L - L_0) \sin(4i_{l0})) / \cos(4i_{l0}), \quad (2)$$

where $L_0 = h_0 / \tan(4i_{l0})$ is the axial distance from the surface intersection to the focus of rays that hit the primary-secondary intersection ring. The best focus location is chosen so that the focused energy on both sides of the focal plane is equal. This corresponds to primary mirror radial height

$$h_{lc} = \sqrt{(h_{lmax}^2 + h_{lmin}^2) / 2} \quad (3)$$

where h_{lmax} and h_{lmin} are the maximum and minimum radial heights of the primary mirror.

Two parameters are needed to design a cone-cone telescope. We start with the L and i_{l0} parameters. The L parameter defines the axial distance from the focal plane to the intersection of the surfaces and the i_{l0} parameter defines the grazing angle of the primary mirror. The radial height at the intersection of the surfaces is approximately:

$$h_{0i_approximation} = L \tan(4i_{l0}) \quad (4)$$

The exact solution for h_0 can be derived from Eq. (2) by substituting h_{lc} for h_l and 0 for the image height H . The solution is:

$$h_0 = \frac{-B + \sqrt{B^2 - AC}}{A}, \quad (5)$$

where A , B , and C are expressed as functions of basic parameters L and i_{l0} and dimensional parameters L_l and c_l . The A , B , and C parameters are:

$$A = 1 - (1 - \cos(4i_{l0}))^2 \quad (6)$$

$$B = \left(\frac{L_l}{2} + c_l\right) \tan(i_{l0}) - L \sin(4i_{l0})(1 - \cos(4i_{l0})) \quad (7)$$

$$C = \frac{[(L_l + c_l)^2 + c_l^2] \tan^2(i_{l0})}{2} - L^2 \sin^2(4i_{l0}). \quad (8)$$

After h_0 is known, the mirror dimensions can be calculated from Eq. (1). To avoid on-axis vignetting, the dimensional parameters L_2 and c_2 have to be chosen so that the on-axis rays intersecting the primary mirror will also intersect the secondary mirror.

3. Surface Equations of Equal-Curvature Telescope

To improve the on-axis focusing capability of the cone-cone telescope, we add axial sag to the cone surfaces. For grazing incidence mirrors the sag is very small and can conveniently be approximated by using a spherical axial profile. This profile is then rotated about the optical axis to produce the surface of revolution. A cross-sectional view of the resulting surfaces is illustrated in Figure 1. Assuming spherical cross-section and the same radius of curvature (R) on the primary and secondary, the surface equations of the primary mirror ($j=1$) and secondary mirror ($j=2$) in the body centered coordinate system of the cones are:

$$h_{j_sph} = h_{j0} - R \cos(i_{j0}) + \sqrt{R^2 - (z_{j_sph} + R \sin(i_{j0}))^2} \quad (9)$$

Since the radius of the spherical surface is very large compared to the axial coordinate, equation can be approximated as:

$$h_{j_sph} \approx h_{j0} - z_{j_sph} \tan(i_{j0}) - \frac{z_{j_sph}^2}{2R \cos^3 i_{j0}} \quad (10)$$

Third and higher order terms in z_{j_sph} are dropped in the expansion. Equation (10) is simply the equation of a cone with a second order correction added to the cone surface. The design and analysis of EC telescopes is based on Eq. (10). The surface equations of the EC telescope can now be abbreviated by:

$$h_j = h_{j0} + a_{1j} z_j + a_{2j} c z_j^2, \quad (11)$$

where $a_{1j} = -\tan(i_{j0})$, $a_{2j} = 1/(2 \cos^3(i_{j0}))$, and $c = \text{curvature of the surfaces } (=1/R)$.

4. Design parameters for Curvature- Telescopes

To design an EC telescope the coefficients of the surface equations need to be described in terms of more convenient system parameters. For x-ray telescopes best choices are the radial height at the surface intersection of the mirrors, the grazing angles at the intersection of the mirrors and the telescope axial length. There are 6 coefficients in the surface equations of the primary and secondary. As for the cone-cone telescope, we select the grazing angle i_{10} of the primary mirror and the axial focal length L of the telescope to be our input parameters. We also require that the grazing angles of the primary and secondary at the surface intersection of the primary and secondary mirror are equal. Under this condition $a_{12} = -\tan(3 i_{10})$ and $a_{22} = 1/(2 \cos(3 i_{10}))$. The radial height h_0 at the surface intersection point and the curvature c of the surfaces are derived from the focusing requirement we set for the telescope.

Curvature c can be solved from the minimum on-axis image requirement. To find the equations for the minimum on-axis image blur, approximate transverse ray equations are first derived for the system. The design is symmetric about the optical axis and only an arbitrary on-axis ray is traced and an equation for the radial component of the ray at the image plane is derived. The radial height (H) of an on-axis ray in terms of $H_0 = (h_0 - L \tan(4i_{10}))$, i_{10} , R , and L is:

$$H = H_0 + z_1[-i_{10} - \frac{25}{3}i_{10}^3 + cL(4 + 66i_{10}^2)] + cz_1^2(-\frac{1}{2} + \frac{8cL}{i_{10}}). \quad (12)$$

Only the second order terms in z_I are kept in Eq. (12). Terms up to third order in i_{10} are kept in the first order z_I -coefficient and -1^{st} and 0^{th} order terms are kept in z_I^2 -coefficient. Eq. (12) is derived in Appendix A. Higher order terms in the expansion are negligible since grazing angle i_{10} is typically small (~ 1 degree) and radius of curvature ($1/c$) of the mirrors is very large (1-10 km)

Curvature c could be calculated from Eq. (12) by deriving first the RMS value of the radial image height and, then, solving the equation for curvature c . A simpler derivation is shown in this paper. Since Eq. (12) is quadratic in z_I the image radial height goes through minimum when the primary mirror axial coordinate z_I changes from its maximum value to its minimum value. Assuming that the minimum H value occurs at the primary mirror axial center point ($z_I = -L_I/2 - c_I$), then, by taking the derivative of Eq. (12) with respect to z_I and solving for c , we find:

$$c = \frac{i_{10} - \frac{49}{6}i_{10}^3}{4L} + \frac{3i_{10}(\frac{L_I}{2} + c_I)}{16L^2}. \quad (13)$$

In Eq.(13) only the 2^{nd} order (L/L) terms are kept and also i_{10} terms up to 3^{rd} order are kept in the first part of the equation and up to 1^{st} order in the second part of the equation.

Approximate solution for the h_0 parameter can be found from Eq. (13). Since Eq. (13) is quadratic, image radial height should reach 0 value when $z_{I1} = -L_I/4 - c_I$ or $z_{I2} = -3L_I/4 - c_I$. Using the first root we find for h_0 :

$$h_0 = L \tan(4i_{10}) + z_{11}[i_{10} + \frac{25}{3}i_{10}^3 - cL(4 + 66i_{10}^2)] + cz_{11}^2(\frac{1}{2} - \frac{8cL}{i_{10}}). \quad (14)$$

5. Surface Equations of OSAC

We used the Optical Surface Analysis Code (OSAC) to ray trace the resulting optical designs. In the OSAC program the surface equations of grazing incidence design are given in the body centered coordinate system (ρ_j, z_j) shown in Figure 1 in the following format:

$$\rho_j = \sqrt{\rho_{0j}^2 + 2K_j z_j - P_j z_j^2}, \quad (15)$$

where ρ_{0j} is the radial height at the axial midpoint of the surface, and K_j and P_j are constants. A second-order correction term can be added to the base surface using OSAC's Legendre polynomials. The second order Legendre term is:

$$sag_j = \frac{d_{2j}}{2} (3(\frac{2z_j}{L_j})^2 - 1), \quad (16)$$

where L_j is the axial length of the surface and d_{2j} is a constant.

The OSAC parameters for cone surfaces can be simply calculated from Eq.(1) by squaring the equation and, then, relating the parameters with the parameters of Eq.(15).

The OSAC input parameters for the EC telescope can now be expressed using Eqs.(15) and (16). The parameters are derived from Eqs.(1) and (11) by translating the

origin of the coordinate to the body centered coordinate system of the surface. The results for the surface parameters are:

$$d_{2j} = -\frac{L_j^2}{12R \cos^3(i_{j0})} \quad (17)$$

$$\rho_{0j} = A_{1j} + \frac{d_{2j}}{2} \quad (18)$$

$$K_j = -A_{2j} \left(A_{1j} + \frac{d_{2j}}{2} \right) \quad (19)$$

$$P_j = -A_{2j}^2, \quad (20)$$

where

$$A_{1j} = h_0 \pm \left(\frac{L_j}{2} + c_j \right) \tan(i_{j0}) - \frac{\left(\frac{L_j}{2} + c_j \right)^2}{2R \cos^3(i_{j0})} \quad (21)$$

$$A_{2j} = \tan(i_{j0}) \pm \frac{\frac{L_j}{2} + c_j}{R \cos^3(i_{j0})} \quad (22)$$

In Eqs. (21) and (22) the upper sign refers to primary mirror ($j=1$) and the lower sign refers to the secondary mirror ($j=2$).

6. Design and Performance of Equal-Curvature Telescope

We have studied EC telescope designs that closely match the size of the Constellation-X SXT telescopes. For this paper we selected two designs from the nested set of Constellation-X telescopes. The basic dimensions and parameters are listed in Tables 1

and 2 for both the EC and equivalent W telescopes. The radial heights of these designs at the primary-secondary intersection plane are 800 mm and 200 mm. The W designs are equivalent with the EC designs in the sense that they have the same radial height h_0 at the surface intersection point and the same axial focal length L .

The shape of the axial profile of the EC telescope is purely second-order in z_j (see Eq.(16)). The axial sag varies from $-d_2/2$ to d_2 along the optical axis from the center of the surface to the maximum or minimum axial value. The d_2 coefficient is slightly larger for the secondary mirror. This is because the sag was designed so that the radius of curvature (R) on both surfaces would be equal. The radii of curvature of the EC design #1 and #2 are 1.98 km and 7.90km, respectively!

In Figure 2 we plot radial height difference between the EC and W telescopes. At the primary-secondary intersection point there is no height difference. Moving towards the front of the primary or towards the back of the secondary, the height differences increase to $0.7 \mu\text{m}$ and $0.2 \mu\text{m}$ for the designs #1 and #2, respectively.

The axial profiles of the EC designs are nearly spherical. The maximum radial height difference between EC equations (Eq.(11)) and spherical profiles (Eq. (9)) is negligible since the third and higher order terms dropped in Eq.(11) would be very small. These terms are proportional to $(z_j/R)^n$ where R is many orders of magnitude larger than z .

Ray trace results indicate that the derived equations do not perfectly predict the location of the on-axis best focus. The focus location is off $4.7 \mu\text{m}$ and $5.7 \mu\text{m}$ for the EC designs #1 and #2, respectively. The small error in the focus location is due to the approximations in the derivation of the curvature.

In Figure 3 the RMS spot diameter is plotted as a function of half-field angle at the gaussian focal plane for the telescopes. Dash curve plots the spot diameter for the EC design #1 and the dash-dot curve plots the spot size for the W design #1. The W design provides slightly improved performance across the field. The on-axis RMS spot diameter of the EC telescope is 0.2 arc-seconds. The performance of EC design #2 and W design #2 is practically the same across the field-of view. The on-axis image diameter of the EC telescope #2 is 0.05 arc-seconds.

The RMS image diameters at the best focal surface are shown in Figure 4. The RMS spot diameters behave similarly. For both designs #1 and #2, W telescope slightly outperforms the EC telescope. If we were to take into account manufacturing tolerances and alignment requirements (half power diameter of 15 arc-second for Constellation-X telescopes), no differences in the telescope performance could be seen.

7. Conclusions

The on-axis and off-axis optical performance of the EC telescopes is surprisingly good compared to the equivalent W type1 telescope. For the grazing angles close to 1 degrees W designs are slightly better in terms of RMS spot diameter and for the grazing angles around 0.3 degrees or smaller there is no practical difference in the optical performance between the telescopes.

The EC telescopes have several advantages over the W telescopes. They are easier to manufacture since the axial profiles are spherical. The polishing tools can be shaped to closely match the surface. The superpolishing of the spherical surface should be easier resulting in smoother surface quality and reduced microroughness.

We believe that the EC designs can be very cost effective. Since the primary and secondary mirror have the same axial sag, a single mandrel could be used to replicate both primary mirror and secondary mirror segments for the CSX/SXT telescopes. This would cut in half the mandrels needed for the project.

The off-axis performance of the designs could be improved by not optimizing the on-axis image size as done in this study, but optimizing a specific off-axis image location. Another way of improving the off-axis performance is to let the curvature vary either on the primary or on the secondary. The resulting telescope would not be an EC design. We will explore these options in the future.

Appendix A: Derivation of Radial Image Coordinate

To derive the radial image coordinate we need to analytically trace a ray through the telescope and solve the equations for the image coordinate. Figure 1 illustrates the principle. A ray hits the primary at a point P. The coordinates and slope angle at this point are h_1 , z_1 , and i_1 . The reflected ray makes an angle $2i_1$ with the optical axis. After the reflection the ray hits the secondary at a point S. The coordinates and slope at this point are h_2 , z_2 , i_2 . After the reflection the ray strikes the focal plane at point H .

Assuming that the primary mirror ($j=1$) and secondary mirror ($j=2$) have equal amount of curvature on their axial profiles, then, the surfaces can be expressed in the telescope coordinate system as:

$$h_j = h_0 + a_{1j}z_j + a_{2j}cz_j^2. \quad (A1)$$

The coordinate system is centered on optical axis at the intersection plane of the mirrors. The a_{1i} and a_{2j} coefficients are defined in Eq.(12). The axial slope angle i_j of the surfaces is just the derivative of Eq. (A1)

$$\tan(i_j) = -a_{1j} - 2a_{2j}cz_j. \quad (\text{A2})$$

To simplify the derivation we express the surface equations in parametric form as a function on quantity

$$\Delta i_j = i_j - i_{j0}, \quad (\text{A3})$$

where i_l is the slope angle of the primary mirror and i_{l0} is the slope angle of the primary at the primary-secondary intersection point. We can solve Eq. (A2) for the primary mirror axial coordinate and similarly write an equation for the secondary mirror:

$$cz_j = \Delta i_j \left(1 - \frac{i_{j0}^2}{2}\right) + \Delta i_j^2 i_{j0} \quad (\text{A4})$$

The slope angle of the secondary $i_{20} = 3i_{10}$. In Eq. (A4) we have expanded trigonometric i_{j0} terms and kept terms up to 3rd order in first order Δi_j term and first order in second order Δi_j . The same approximations will be applied to all the equations presented below. The radial coordinates h_j can be derived by substituting Eq. (A4) into Eq.(11), keeping only 2nd order terms in Δi_j and expanding the coefficients. We get:

$$ch_j = -\Delta i_j (i_{j0} - i_{j0}^3) - \Delta i_j^2 \frac{1}{2}. \quad (\text{A5})$$

First, we need to derive for the traced ray the secondary mirror coordinates as a function of the primary mirror coordinates. Since we know the slope angle of the reflected ray we can write an equation:

$$h_1 + z_1 \tan(2i_1) = h_2 + z_2 \tan(2i_1). \quad (\text{A6})$$

Deriving approximated equation for $\tan(2i_1)$ and substituting the resulting equation and Eqs.(A4) and (A5) into Eq.(A6), we solve Eq.(A6) for Δi_2

$$\Delta i_2 = -\Delta i_1 - \frac{\Delta i_1^2}{i_{10}} 4. \quad (\text{A7})$$

Substituting Eq. (A7) into secondary mirror equations (A4) and (A5) we find for z_2 and h_2 :

$$cz_2 = -\Delta i_1 \left(1 - \frac{9}{2} i_{10}^2\right) - \Delta i_1^2 \frac{4}{i_{10}} \quad (\text{A8})$$

$$c(h_2 - h_0) = \Delta i_1 \left(3i_{10} - \frac{9}{2} i_{10}^3\right) + \Delta i_1^2 \frac{23}{2}. \quad (\text{A9})$$

Tracing the ray from the secondary to image plane gives us an equation for the radial image coordinate:

$$H = h_2 - (L - z_2) \tan(\alpha), \quad (\text{A10})$$

where $\alpha (=2\Delta i_2 - 2\Delta i_1)$ is an angle between reflected ray after second reflection and optical axis. After deriving an equation for $\tan(\alpha)$ and substituting Eqs. (A8) and (A9) into Eq.(A10), we get:

$$H - H_0 = \Delta i_1 \left[R(-i_{10} - \frac{47}{6} i_{10}^3) + L(4 + 64i_{10}^2) \right] + \Delta i_1^2 \left[-\frac{R}{2} + \frac{8L}{i_{10}} \right], \quad (\text{A11})$$

where $H_0 = h_0 - L \tan(4i_{01})$. Finally, solving Eq.(A4) for Δi_1 and substituting into Eq. (A11) we get the radial image height as a function of primary mirror axial coordinate z_1 :

$$H = H_0 + cz_1 \left[R(-i_{10} - \frac{25}{3} i_{10}^3) + L(4 + 66i_{10}^2) \right] + c^2 z_1^2 \left(-\frac{1}{2} + \frac{8cL}{i_{10}} \right). \quad (\text{A12})$$

Figure Captions.

Figure 1. Cross-section of the cone-cone telescope. Dashed curves represents the axial curvature added to the surfaces to modify the cone-cone design to the Equal-Curvature design. Primary-secondary intersection plane and optical axis defines the telescope coordinate system. Primary BCC and Secondary BCC define the body centered coordinate system for the mirrors.

Figure 2. Radial height difference between the Equal-Curvature telescopes and equivalent Wolter telescopes in the body centered coordinate system. Solid line and dotted line represents the height difference of the primaries and secondaries of the design #1. Dashed line and dot-dash line represents the height difference between the primaries and secondaries of the design #2.

Figure 3. RMS spot diameter as a function of the half-field angle for the Equal-Curvature and equivalent Wolter telescopes at Gaussian focal plane. Dash line and dot-dash line represent EC and W designs #1. Solid line and dotted line represent EC and W designs #2.

Figure 4. RMS spot diameter as a function of the half-field angle for the Equal-Curvature and equivalent Wolter telescopes at best focal surface. Dash line and dot-dash line represent EC and W designs #1. Solid line and dotted line represent EC and W designs #2.

Table 1. Basic design parameters for the Equal-Curvature telescopes and equivalent Wolter telescopes.

Telescope	i_{10} (deg)	h_0 (mm)	L (m)	L_1 and L_2 (mm)	c_1 (mm)	c_2 (mm)
EC #1	1.14344537	800	10	300	25.1	24.9
EC #2	0.28643407	200	10	300	25.1	24.9
Wolter #1	1.14348032	800	10	300	25.1	24.9
Wolter #2	0.28644711	200	10	300	25.1	24.9

Table 2. OSAC parameters for the Equal-Curvature telescopes and equivalent Wolter telescopes.

Telescope	ρ_{01} (mm)	ρ_{02} (mm)	K_1 (mm)	K_2 (mm)	P_1 ($\times 10^{-5}$)	P_2 ($\times 10^{-4}$)	d_{21} (μm)	d_{22} (μm)
EC #1	803.4853212	789.5063679	-15.96638166	-47.39512177	-39.48727085	-36.03761259	-3.7812	-3.7994
EC #2	200.8729557	197.3743029	-0.999763061	-2.964744897	-2.47714389	-2.256282328	-0.9495	-0.9498
Wolter #1	803.4874205	789.5080282	-15.96811725	-47.39674315	0.0	-31.93619384	-	-
Wolter #2	200.8734835	197.3747161	-0.9.99875031	-2.964849407	0.0	-1.999750054	-	-

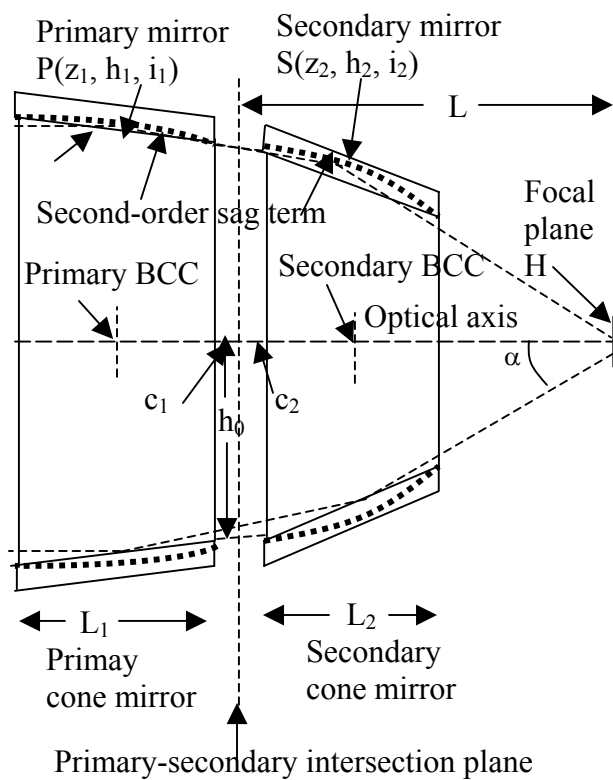


Figure 1.

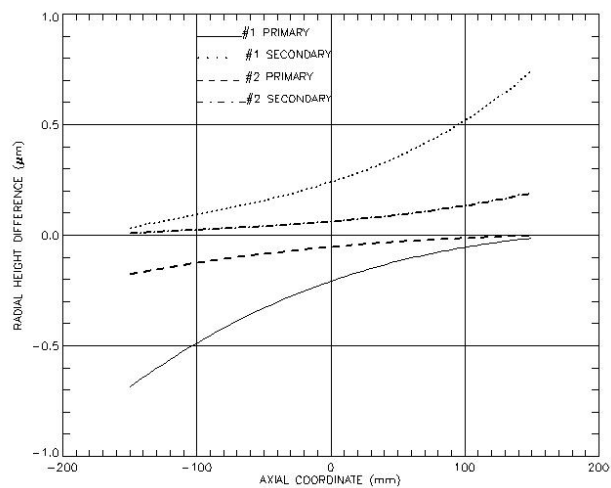


Figure 2.

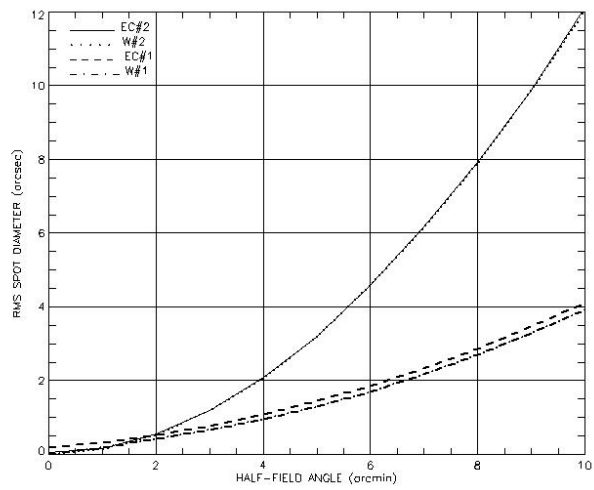


Figure 3.

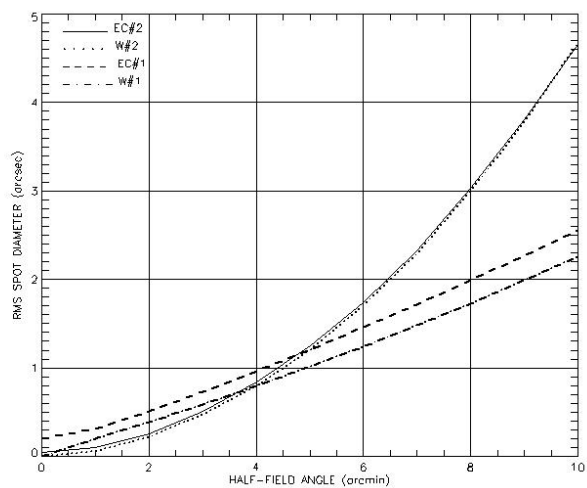


Figure 4.

8. References

-
- ¹ N.E.White and H.Tannanbaum,"The constellation-X-ray mission", in *New Century of X-ray Astronomy*, H.Inoue and H.Kuneida, Eds., ASP Conference Proc, **251**, 224-229 (2001).
- ² W. A. Podgorski, D. Content, P. Glenn, J. Hair, R. Petre, T. Saha, M. Schattenburg, J. Stewart, and W. Zhang, "Constellation-X soft x-ray telescope assembly and alignment, in *X Ray and Gamma Ray Telescopes and Instruments for Astronomy*, J. E. Truemper and H. D. Tannanbaum, Eds. "Proc. SPIE, **4851**, 491-502 (2002).
- ³ H. Wolter, "Mirror systems with glancing incidence on image producing optics for x-rays, " *Ann. Phys.* **10**, 94-114 (1952).
- ⁴ T.T.Saha, "Transverse ray aberrations of Wolter type 1 telescopes, "in *Grazing Incidence Optics*, J.F.Osantowski and L.P VanSpeybroeck, eds, Proc. SPIE, **640**, 10-19 (1986).
- ⁵ J.D. Mangus and J.H. Underwood, "Optical design of glancing incidence x-ray telescope, " *Appl. Opt.*, **8**, 95-102 (1969).
- ⁶ L. P. VanSpeybroeck and R. C. Chase, "Design parameters of paraboloid-hyperboloid telescopes for x-ray astronomy," *Appl. Opt.* **11**, 440-445 (1972).
- ⁷ H. Wolter, "Generalized Schwarzschild mirror systems with glancing incidence as optics for x-rays, " *Ann. Phys.* **10**, 286-295 (1952).
- ⁸ R. C. Chase and L. P. VanSpeybroeck, "Wolter-Schwarzschild telescopes for x-ray astronomy," *Appl. Opt.* **12**, 1042-1044 (1973).
- ⁹ R. Petre and P. J. Serlemitsos, "Conical imaging mirrors for high-speed x-ray telescopes," *Appl. Opt.* **24**, 1833-1836 (1985).
- ¹⁰ P. J. Serlemitsos, "Conical foil x-ray mirrors: performance and projections, " *Appl. Opt.* **27**, 1447-1452 (1988).
- ¹¹ W. Werner, Imaging properties of Wolter I type x-ray telescopes, " *Appl. Opt.* **16**, 764-773 (1977).
- ¹² C.J. Burrows, R. Burg, and R. Giacconi, "Optimal grazing incidence optics and its application to wide-field x-ray imaging," *Astrophys. J.* **392**, 760-765 (1992).
- ¹³ P. Conconi and S. Campana, "Optimization of grazing incidence mirrors and its application to surveying x-ray telescopes," *A&A*, **372**, 1088-1094 (2001).
- ¹⁴ K. Nariai, "Geometrical aberration of a generalized Wolter type I telescope, " *Appl. Opt.* **26**, 4428-4432 (1987).
- ¹⁵ K. Nariai, "Geometrical aberration of a generalized Wolter type I telescope. 2: analytical study, " *Appl. Opt.* **27**, 345-350 (1988).
- ¹⁶ J. E. Harvey, A. Krywonos, P.L.Thompson, and T.T.Saha, "Grazing-incidence hyperboloid-hyperboloid designs for wide-field x-ray imaging applications, " *Appl. Opt.* **40**, 136-144 (2001).
- ¹⁷ R. J. Noll, P. Glenn, and J. F. Osantowski, "Optical Surface Analysis Code (OSAC), in *Scattering in Optical Materials II*, S. Musikant, ed, Proc. SPIE, **362**, 78-82 (1983).